Estuarine, Coastal and Shelf Science (2001) **52,** 33–49
doi:10.1006/ecss.2000.0726, available online at http://www.idealibrary.com on IDEAL®

Modelling Oxygen Dynamics in an Intermittently Stratified Estuary: Estimation of Process Rates Using Field Data

M. E. Borsuk[a], C. A. Stow[a], R. A. Luettich, Jr.[b], H. W. Paerl[b] and J. L. Pinckney[c]

[a]*Nicholas School of the Environment, Duke University, P.O. Box 90328, Durham, NC 27708-0328, U.S.A.*
[b]*Institute of Marine Sciences, University of North Carolina at Chapel Hill, 3431 Arendell Street, Morehead City, NC 28557, U.S.A.*
[c]*Department of Oceanography, Texas A & M University, College Station, TX 77843-3146, U.S.A.*

Received 16 March 2000 and accepted in revised form 22 September 2000

The relationship between bottom water dissolved oxygen concentration, vertical stratification, and temperature was investigated for the Neuse River estuary, North Carolina, a shallow, intermittently-mixed estuary using approximately 10 years of weekly/biweekly, mid-channel data. A generalized additive model (GAM) was used to initially explore the major relationships among observed variables. The results of this statistical model guided the specification of a process-based model of oxygen dynamics that is consistent with theory yet simple enough to be parameterized using available field data. The nonlinear optimization procedure employed allows for the direct estimation of microbial oxygen consumption and physical reoxygenation rates, including the effects of temperature and vertical stratification. These estimated rates may better represent aggregate system behaviour than closed chamber measurements made in the laboratory and *in situ*. The resulting model describes 79% of the variation in dissolved oxygen concentration and is robust when compared across separate locations and time periods. Model predictions suggest that the spatial extent and duration of hypoxia in the bottom waters of the Neuse are controlled by the balance between the net oxygen depletion rate and the frequency of vertical mixing events. During cool months, oxygen consumption rates remain low enough to keep oxygen concentration well above levels of concern even under extended periods of stratification. A concentration below 4 mg l^{-1} is only expected under extended periods without vertical mixing when bottom water temperature exceeds 15 °C, while a concentration below 2 mg l^{-1} is only expected when water temperature exceeds 20 °C. To incorporate the effects of parameter uncertainty, model error, and natural variability on model prediction, we used Monte Carlo simulation to generate distributions for the predicted number of days of hypoxia during the summer season. The expected number of days with a dissolved oxygen concentration less than 4 mg l^{-1} is 46·8 with a standard deviation of 4·7, while 23·8 days are expected to have an oxygen concentration below 2 mg l^{-1} with a standard deviation of 4·2 days. When joined with models relating nutrient loading and productivity to benthic and pelagic respiration rates, this model will be useful for probabilistically predicting the impact of nutrient management on the frequency of low oxygen events.

Keywords: oxygen dynamics; hypoxia; respiration; modelling; rate estimation; uncertainty analysis; Neuse River

Introduction

Oxygen deficiency is a serious problem in many estuaries and coastal waters (Diaz & Rosenberg, 1995). Documented impacts of hypoxia on aquatic organisms include reduced habitat availability, increased susceptibility to disease and predation, and direct kill events (Pihl *et al.*, 1992; Dauer *et al.*, 1992; Winn & Knott, 1992). Oxygen depletion in estuarine bottom waters results from chemical and biological oxygen consumption associated with the decomposition of organic matter in the sediments and water column. Sources of organic matter may include external watershed loading or internal nutrient-driven algal production (Paerl *et al.*, 1998). In an effort to control hypoxia and its detrimental effects, many coastal states are proposing watershed management actions intended to reduce benthic and pelagic oxygen demand by limiting nutrient loading and resultant algal stimulation. However, the severity of oxygen depletion in the bottom water of estuaries depends on several factors in addition to oxygen demand, including frequency of mixing, vertical density stratification, and exchange of oxygen with the surface layer. In deep estuaries, or those for which mixing is controlled by spring-neap tidal cycles, large areas of hypoxic bottom water may persist for weeks or even months (Officer *et al.*, 1984). However, in shallow estuaries, vertical mixing due to wind and river flow occurs frequently enough to control the spatial and temporal extent of

0272–7714/01/010033+17 $35.00/0

low oxygen events (Turner *et al.*, 1987). Given the important role that physical factors play in determining the frequency and extent of hypoxia, the impact of nutrient reduction is likely to be highly nonlinear (Kemp *et al.*, 1992; Lohrenz *et al.*, 1997). Therefore, understanding the interplay between respiration, reoxygenation, and the timing of mixing events is important to predicting estuarine response to proposed management actions.

Previous efforts at estuarine oxygen modelling have focused on deeper bays with seasonal or spring tide mixing (Kemp & Boynton, 1980; Officer *et al.*, 1984; Kuo *et al.*, 1991; Kemp *et al.*, 1992). While the relatively long time scale of mixing processes in these systems has facilitated the estimation of oxygen budgets, such models were not developed to predict estuarine response to changed conditions. A difficulty in using these models to inform long-term management decisions has been their reliance on detailed processes with many unobservable rates and parameters. While such highly mechanistic models may be conceptually appealing, practically they make confidence in the parameter selection process difficult (Reckhow, 1994*a*). System-specific field data at the appropriate level of detail generally does not exist for even the most highly studied estuaries. As a result, modellers have either had to resort to using tabulated values derived from a variety of aquatic systems (Officer *et al.*, 1984), rely on the results of controlled laboratory incubations (Kemp *et al.*, 1992), or limit the interpretation of their models to hypothetical diagnostic studies (Kuo *et al.*, 1991).

For periodically-mixed estuaries in which oxygen patterns are controlled on shorter time scales, the quantification of process rates and parameters is even more challenging, and oxygen modelling has been limited to simple approximations (Turner *et al.*, 1987; Stanley & Nixon, 1992). While these predictions may provide first estimates, their assumptions of consistency and linearity may not be appropriate, and they were not developed to elucidate expected changes in response to management. Additionally, neither the highly mechanistic nor the very simplistic approaches have provided estimates of the inherent uncertainty resulting from both natural variability and model error. This lack of uncertainty information makes it difficult to evaluate candidate models based on their predictive ability and reduces the models' utility for rational environmental management and decision-making (Reckhow, 1994*b*).

An alternative to previous efforts at estuarine modelling is to allow the scale of model specification to be determined by the availability of relevant observational data (Reckhow, 1999). Thus, model process rates and parameters can be derived using existing field data. This approach can be expected to produce relatively simple models that achieve a practical compromise between complexity and utility. Such models will likely focus on predicting aggregate system behaviour rather than fine detail. Prediction of aggregate response to large scale management actions is generally consistent with the needs of decision-makers (Walters & Holling, 1990; Reckhow, 1999) and has the additional advantage of being well supported by site specific observation. Simpler models that are empirically parameterized can also be practically subjected to a rigorous uncertainty analysis and are more easily communicated to decision-makers and stakeholders involved in the management process.

We describe the development of a predictive oxygen model for the Neuse River estuary, North Carolina. Because of the empirical nature of our approach, our modelling methodology relies on the results of data analysis and statistical exploration. Therefore, we deviate slightly from the conventional organizational structure in this paper. We begin with a description of the study site and sampling protocol, followed by an analysis of the patterns of interannual and seasonal variation for observed variables expected to control oxygen concentration. We then explore the major relationships among these variables using a generalized additive model (GAM). Based on these results, a process-based model of oxygen depletion is specified that is consistent with established theory yet is simple enough to be empirically parameterized using least squares optimization. This formulation has the advantage over a strictly empirical model, such as the GAM, in that process rates related to benthic respiration and vertical reoxygenation are explicitly estimated. These rates based on field data are easier to estimate and may better represent aggregate system behaviour than closed chamber measurements made in the laboratory or *in situ*. Model results suggest additional simplification which lend insight into system behaviour and improve computational efficiency. Parameter and model uncertainty, as well as natural variability, are then incorporated into the model using Monte Carlo simulation to generate probabilistic predictions about the frequency of hypoxic conditions. The ecological significance of the predictions is then discussed, with a focus on extending the approach to other aspects of the estuarine system that are of interest to the public and decision-makers.

Study site

The Neuse River originates north of Durham, NC, and flows approximately 320 km through the central

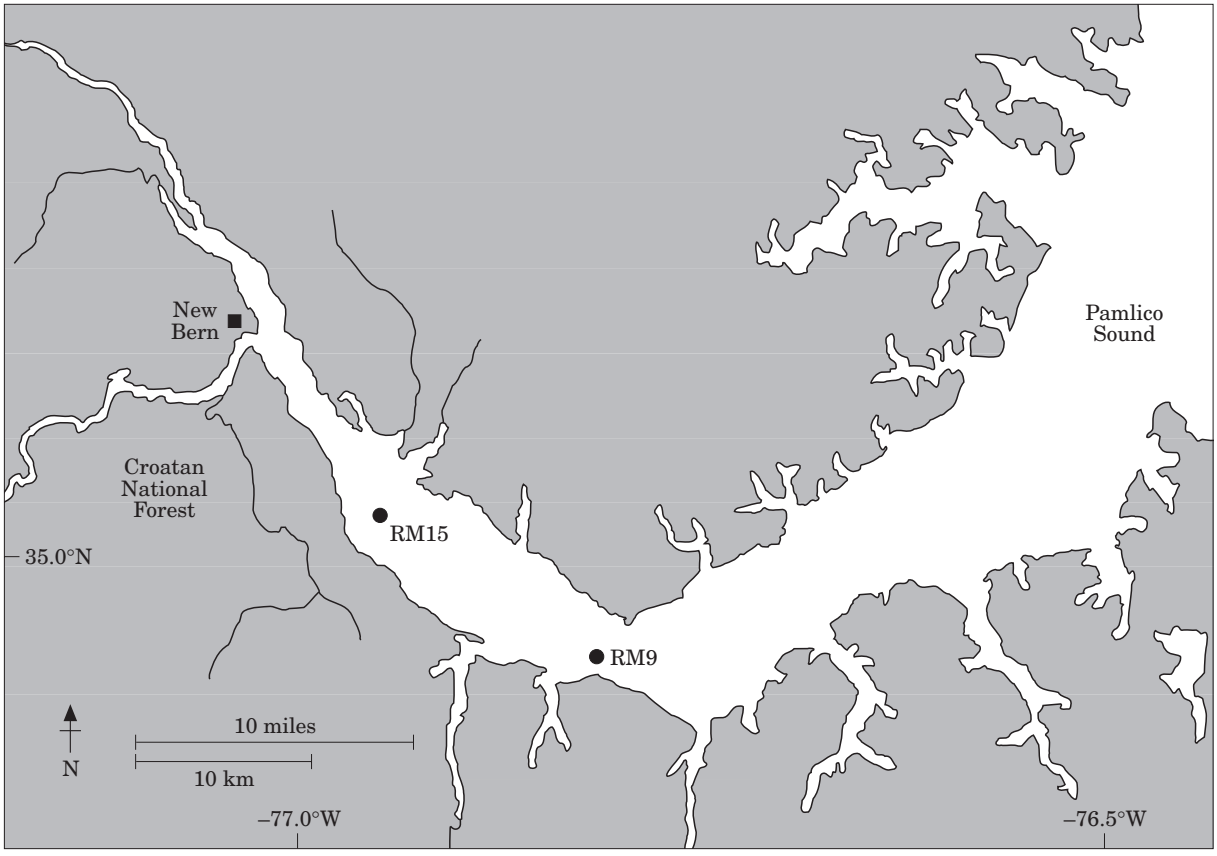

FIGURE 1. Neuse River estuary and location of the mid-channel sampling stations.

piedmont to the coastal plain and comprises a watershed area of 16 108 km^2. The major land uses in the basin are agriculture (35%) and forestry (34%) with the remainder consisting primarily of urban areas, wetlands, scrub, and open water (NC Department of Environment, Health and Natural Resources, 1993). The upper portion of the basin includes much of North Carolina's Research Triangle (defined by the cities of Raleigh, Durham, and Chapel Hill), an area that has experienced economic prosperity and rapid population growth since the 1970s. Population expansion and development are also occurring in lower portions of the basin with an increasing coastal population and a growing commercial hog-farming industry.

The Neuse River estuary (Figure 1) has received considerable attention in recent years due to excessive algal blooms, frequent periods of low dissolved oxygen, and extensive fish kills. These problems have been attributed to the high nutrient loading that generally results from the kinds of changes that have occurred in the watershed over the past several decades (McMahon & Woodside, 1997; Paerl *et al.*, 1995). Nutrient management options, including riparian buffers and best management practices, are being considered to control nutrient inputs, and the establishment of Total Maximum Daily Loads (TMDLs) to further regulate nutrient loads is expected in the near future.

The Neuse Estuary is characterized as an intermittently-mixed estuary (Luettich *et al.*, 1998). The shallow average depth (<4 m) combined with the protection from tides offered by the Outer Banks means that wind is the primary mechanism controlling vertical mixing (Rizzo & Christian, 1996; McNinch & Luettich, 1998). Thus, depending on wind conditions, the estuary may be anywhere from vertically homogeneous to highly stratified. The vertical temperature gradient in the Neuse is generally minor, and density stratification is driven primarily by salinity differences resulting from saltwater intrusion (Christian *et al.*, 1986). Previous studies have noted the correlation between low bottom water oxygen concentration and vertical salinity gradient in the Neuse (Paerl *et al.*, 1998), however this relationship has not been quantified and there are no published attempts to model the oxygen dynamics.

Sampling protocol

Measurements of dissolved oxygen concentration, water temperature, and salinity are part of a long-term data set managed by investigators at the Institute of Marine Sciences (IMS), Morehead City, NC. Data were contributed by researchers at IMS, East Carolina University (ECU), the North Carolina Division of Water Quality (DWQ) and the Weyerhauser Corporation. Sampling consisted of vertical profiles collected at multiple mid-channel locations spanning the gradient from freshwater to saline conditions and were collected at approximately two week intervals for the period March 1985 to February 1989 and January 1994 to May 1997 and weekly from June 1997 to January 1999. Measurements during the first sampling period were obtained using a YSI Model 57 oxygen meter and a YSI Model 33 meter for temperature and salinity (Boyer *et al.*, 1994). During the second period, a HydroLab H20 datasonde probe was used (Paerl *et al.*, 1998). Sampling locations used in the present analysis were chosen based on temporal coverage as well as proximity to areas of oxygen concern. The focus of this study was on a mid-estuarine, mesohaline location identified as River Marker 9 (RM9; Figure 1). Samples were collected at RM9 during both sampling periods and it is in the vicinity of an historically high number of fish kills believed to be due to low oxygen. Average depth at RM9 is 4 m. To examine the generality of the model form and compare the spatial variability of parameter values, the process-based model was also parameterized using the data of River Marker 15 (RM15). RM15 is located approximately 15 km upstream of RM9 (Figure 1) and has an average depth of 3 m. Data were collected at RM15 only during the second sampling period, January 1994 to January 1999.

In addition to the weekly/biweekly samples, this study uses time-series data obtained at a mooring located near RM9. Measurements were taken of temperature, conductivity and salinity (determined from temperature and specific conductance) at near-surface and near-bottom depths. The data were collected using two InterOcean S4 electromagnetic current meters deployed 75 cm above bottom and 75–125 cm below surface. Average water depth at the mooring is 4 m. The mooring was established in August 1997 as part of the Neuse River Estuary Modeling and Monitoring Project (McNinch & Luettich, 1998). The meters were initially programmed for a sampling rate of 2 Hz for 5 min out of every 30 min until June 1998, when the rate was changed to 3 min out of every 15 min. Meters were serviced every 8–10 weeks, and temperature and conductivity measurements were verified with an independently calibrated HydroLab Surveyor 3 and H20 CTD (McNinch & Luettich, 1998).

Observational data analysis

The annual distribution of bottom water dissolved oxygen concentration at RM9 shows no obvious trend over the past 15 years (Figure 2). There is some variability from year to year, however this variation is mainly in the extreme values with the median concentration remaining relatively constant at just over 6 mg l^{-1}. This constancy is also true for the bottom water temperature, the distribution of which has not changed from year to year, even at the extreme values. The salinity gradient (difference between measurements in the bottom and top layers) at this location also shows no clear trend, although the variation in the highest measured values may be substantial.

Dissolved oxygen concentration exhibits a distinct seasonal pattern (Figure 3) characterized by a summer minimum with median values as low as 2 mg l^{-1} in July. Within-month variability also depends on season, with a wider spread in observed values in summer than in winter. Bottom water temperature follows the expected seasonal cycle, with a summer peak and winter trough. Within-month variability is relatively minor and consistent throughout the year. Salinity gradient values show no clear pattern. Neither median values nor extremes show distinct seasonal differences, although within-month variability is high. While the monthly distributions of dissolved oxygen and temperature appear to depend on the time of year, stratification, as measured by salinity gradient, appears to have a consistent underlying distribution throughout the year. Thus, stratification alone is not enough to generate hypoxic conditions, and warm water temperature is likely an important contributing factor.

Data from the continuous monitoring station (Figure 4) show that the salinity gradient is highly variable. However, the time-series record is marked by periods of mixed conditions indicated by a near-zero salinity gradient, followed by periods in which the gradient increases approximately linearly with time. It is likely that these periods of steadily increasing stratification correspond with extended periods of calm wind and flow conditions. Intermittent sharp declines in stratification suggest vertical-mixing events caused by wind or flow changes that return the salinity gradient to near zero. Certainly there is noise superimposed on this piecewise linear pattern, perhaps due partly to winds of insufficient strength to fully mix the

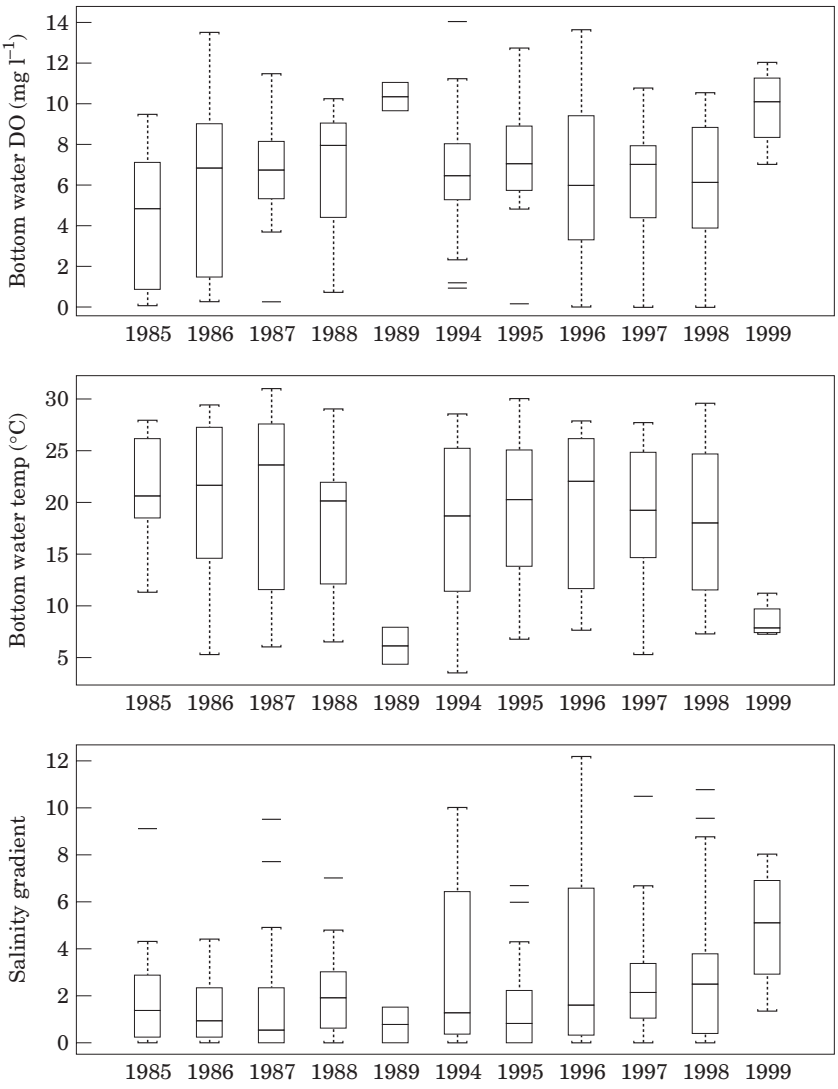

FIGURE 2. Box-and-whisker plots by year of observed values at RM9 for (a) bottom water dissolved oxygen concentration (mg l^{-1}), (b) bottom water temperature (°C), and (c) salinity gradient. The box represents the range of the first and third quartile, the line through the box represents the median, and the whiskers represent outliers within 1·5 times the inter-quartile range. Samples were not collected throughout the full calendar year in 1985, 1989, and 1999, resulting in the incomplete distributions shown in the figure.

system, however the pattern appears consistent and can also be seen in the salinity records of other intermittently mixed estuaries (e.g. Stanley & Nixon, 1992).

Statistical modelling

Statistical modelling methodology

To explore the relationships among the measured variables, we used a generalized additive model (GAM) (Hastie & Tibshirani, 1990; Reckhow & Qian, 1994). GAM methods rely on visualization, bivariate smoothing, and an additive functional form. The method provides a non-parametric alternative to linear regression when the relationship between the response variable and predictors is nonlinear and a parametric relationship is not obvious. In this context, non-parametric does not refer to rank-ordering procedures, such as the Mann-Whitney or Wilcoxon tests, but rather the absence of a parameterized model defining the relationship among observed variables. In a GAM, the traditional linear function of the predictor variables is replaced by a non-parametric smoothing function. This results in the following model form:

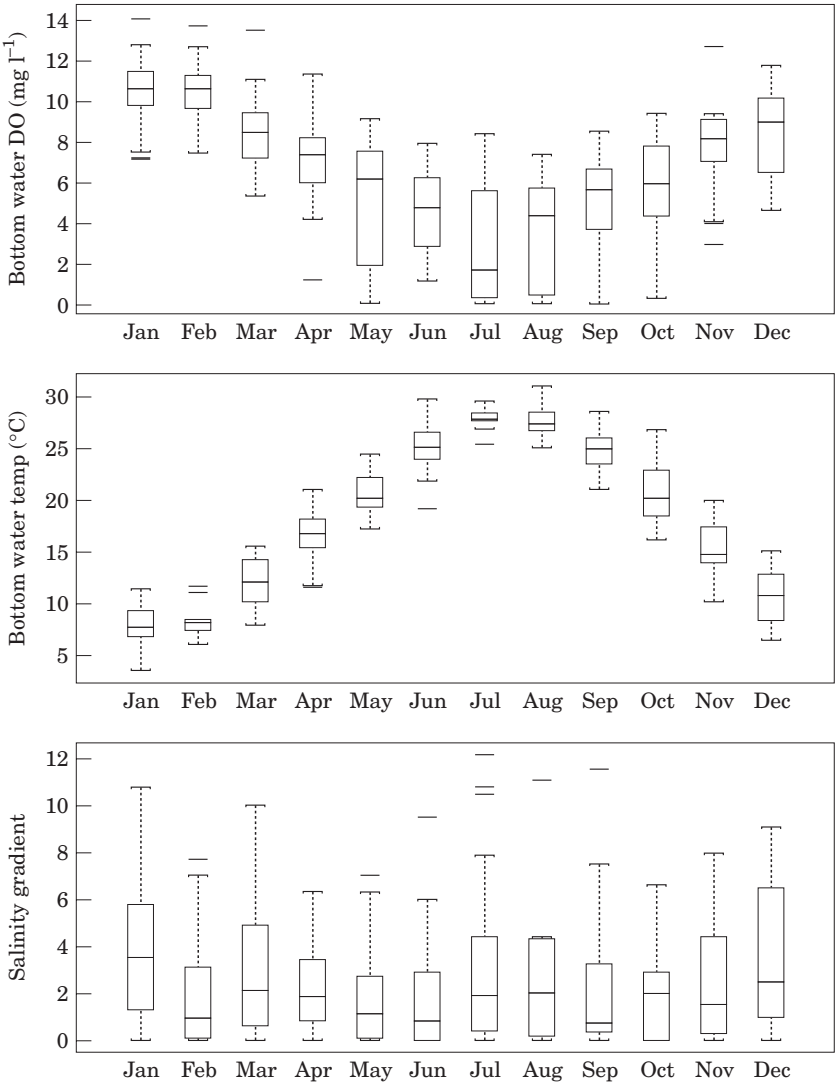

FIGURE 3. Box-and-whisker plots by month of observed values at RM9 for (a) bottom water dissolved oxygen concentration (mg l^{-1}), (b) bottom water temperature (°C), and (c) salinity gradient. The box represents the range of the first and third quartile, the line through the box represents the median, and the whiskers represent outliers within 1·5 times the inter-quartile range.

$$Y = \alpha + \sum_{j=1}^{p} f_j(X_j) + \varepsilon \qquad (1)$$

where α is the overall mean of Y, f_j is a smoothing function for the predictor variable X_j, and ε is an error term. The smoothing functions are estimated iteratively one predictor variable at a time using a back-fitting estimation algorithm. The resultant smoothing function describes locally persistent patterns in the data attributable to each predictor variable. Although the function is non-parametric, plots of smoothing functions together with partial model residuals can aid in data visualization and selection of appropriate functional forms for parametric model construction. We used the version of GAM included with S-Plus® (Chambers & Hastie, 1992) which employs a local error sum of squares smoother.

Statistical modelling results

The results of the GAM fit to the RM9 data with dissolved oxygen as the response variable and salinity gradient and bottom water temperature as the predictors indicate that both variables are important in determining bottom water oxygen concentration (Figure 5). The contribution of water temperature to dissolved oxygen is very nearly linear, with lower expected concentration at high temperature. The

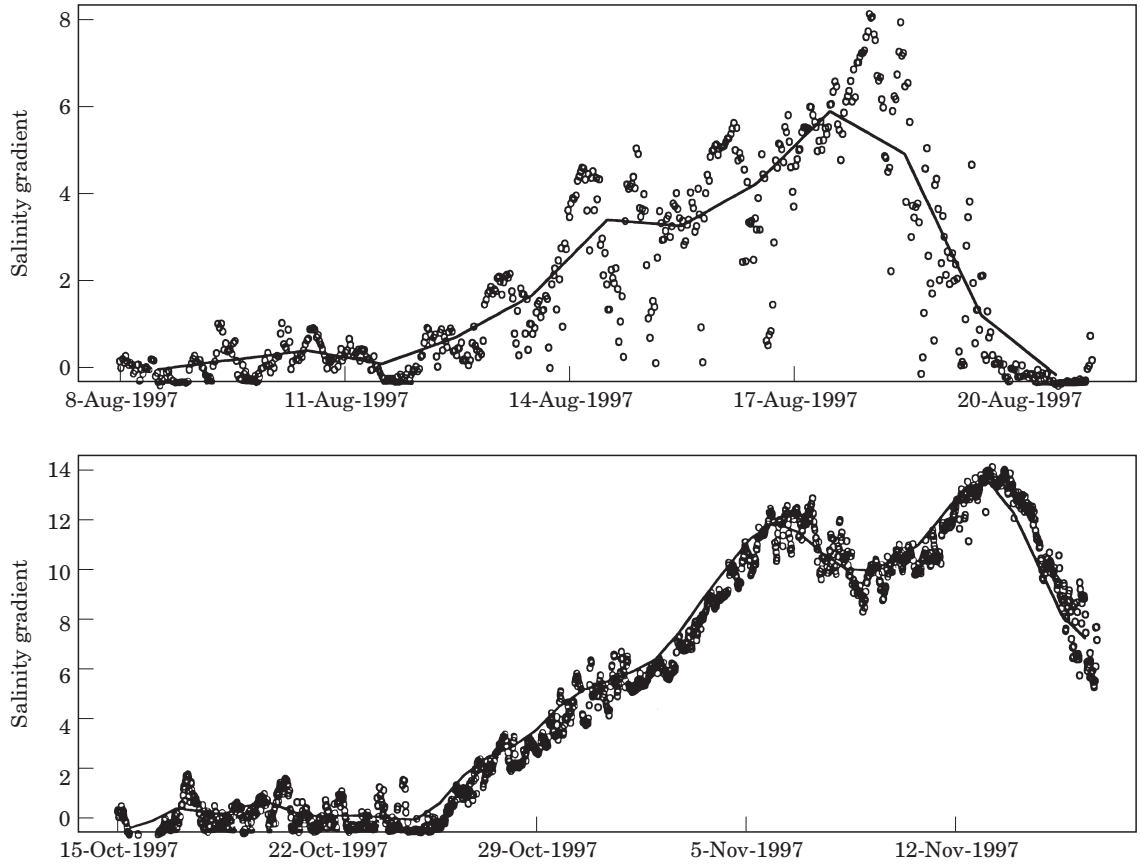

FIGURE 4. Measured salinity gradient for two periods as recorded by the continuous monitoring station near RM9. The points represent measurements taken at 30 min intervals and the lines represent average daily values.

direction of this relationship might be expected based on the effect of temperature on oxygen saturation values, however the magnitude of the temperature effect is greater than twice that expected due to changes in saturation values alone (Hyer *et al.*, 1971). Salinity gradient also has a clear relationship with dissolved oxygen. However this relationship is non-linear with sharp declines in oxygen upon initial increases in gradient and a reduced slope at higher values. This observation suggests that the net rate of oxygen depletion at a fixed temperature is controlled, at least in part, by factors other than the vertical reoxygenation rate. It should also be noted that the distribution of salinity gradient values (Figure 5) does not show a bimodal pattern in which the system is either ' stratified ' or ' not '. Rather, there are many days with a low salinity gradient, and higher values are increasingly rare. This is consistent with the observations from the continuous monitoring data (Figure 4).

Both surface and bottom algal density, as measured by chl *a* on corresponding sampling days, were also initially included as predictor variables in the GAM. Algal photosynthesis and respiration have been shown to exert a significant influence on dissolved oxygen concentration in some estuarine systems (Kemp *et al.*, 1992). However, at RM9 in the Neuse Estuary, bottom water dissolved oxygen did not exhibit any relationship with contemporaneous chl *a* when it was included as a predictor together with salinity gradient and bottom water temperature (not shown). This suggests that net algal respiration, as captured by chl *a* measurements, is relatively minor in the lower portion of the water column in relation to other mechanisms of oxygen depletion, including benthic and water column oxygen uptake by bacteria.

Dissolved oxygen exhibits a close association with salinity gradient and bottom water temperature as revealed by the GAM. Using the square of the correlation between observed and predicted values as a measure of descriptive ability (analogous to R^2 in parametric models), these two predictor variables describe 77·5% of the variation in the response. If predicting oxygen concentration at a specific salinity gradient and temperature were the goal of a modelling effort, this GAM would do very well. However, for guiding management and decision-making, the model

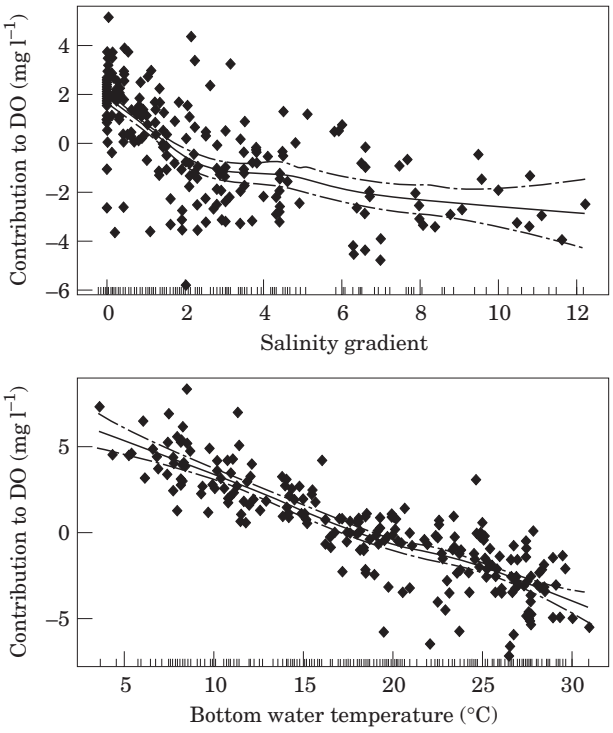

FIGURE 5. Partial residual plots of the smooth functions used in the GAM developed for RM9. The solid lines represent the individual contributions of salinity gradient and bottom water temperature to predicted dissolved oxygen concentration after subtracting the overall mean. The dotted line represents ± one standard error from the mean fitted value. Plotted points in each plot represent the model residuals after accounting for the fitted effect of the other predictor variable. Tick marks along the horizontal axis indicate the distribution of salinity gradient values.

is not very useful. Neither of the predictor variables can be linked to management actions intended to control hypoxia, nor are there specific process rates that can be adjusted based on expected changes. Therefore, the GAM is most useful in guiding the development of the process-based model.

Process-based modelling and empirical rate estimation

Model formulation

Due to the longitudinal extent of hypoxia in the Neuse Estuary (Paerl *et al.*, 1998) and the long water residence times (Christian *et al.*, 1986), we assume that net horizontal oxygen transport is minor for a location in the middle section of the estuary. Therefore, the concentration of dissolved oxygen in a vertically averaged parcel of bottom water can be described by the rate equation:

$$\frac{dC}{dt} = -R_d + R_v \tag{2}$$

where C is the average concentration of dissolved oxygen in the lower water column (mg l^{-1}), t is the time since the last vertical mixing event (d), R_d is the combined benthic and lower water column oxygen demand (mg l^{-1} d^{-1}), and R_v is the vertical oxygen exchange rate from the upper water layer (mg l^{-1} d^{-1}) (Officer *et al.*, 1984). This equation states that the net rate of oxygen concentration change in the bottom water is determined by the relative magnitudes of the consumption rate and the reoxygenation rate across the pycnocline.

At low water velocities, the oxygen demand, R_d, has been found to be linearly related to oxygen concentration according to the expression,

$$R_d = k_d C \tag{3}$$

where k_d is the rate constant (d^{-1}) (Phoel *et al.*, 1981; Moore *et al.*, 1996; Park & Jaffe, 1999). First-order rate constants are generally considered to have a temperature dependency according to the Arrhenius formulation,

$$k_d(T) = k_{d20}\theta_d^{T-20} \tag{4}$$

where T is temperature (°C), k_{d20} is the rate constant at 20 °C, and θ_d is a constant representing the level of temperature dependency (Bowie *et al.*, 1985; Chapra, 1997).

Vertical oxygen exchange in estuaries is generally considered to be dominated by diffusive, rather than advective, processes (Officer, 1976). Therefore the exchange rate can be expressed as proportional to the oxygen concentration gradient across the pycnocline:

$$R_v = k_v(C_u - C) \tag{5}$$

where C_u is the oxygen concentration in the upper layer, and k_v is the vertical exchange coefficient (d^{-1}) (Officer *et al.*, 1984; Kuo *et al.*, 1991; Kemp *et al.*, 1992). Density differences between the surface and bottom layers reduce turbulent kinetic energy and thus can be expected to reduce the vertical exchange coefficient. Munk and Anderson (1948) proposed a modification of k_v according to:

$$k_v = \frac{k_v'}{(1 + aRi)^{3/2}} \tag{6}$$

where k_v' is the exchange coefficient at $Ri = 0$, a is a constant, and

$$Ri = \frac{bouyancy}{shear} = \frac{(g/\rho)\,\partial\rho/\partial z}{(\partial u/\partial z)^2} \tag{7}$$

is the Richardson number where g is the acceleration due to gravity, ρ is the water density, z is depth, and u is horizontal velocity. More complex parameterizations have been developed since Munk and Anderson proposed Equation 6, but we chose this formulation because it is relatively simple and has been found to provide a reasonable estimate of the effect of stratification on vertical exchange (Geyer, 1993).

In the Neuse Estuary, the vertical density gradient is primarily the result of salinity differences. Therefore, we can express the $d\rho/dz$ term in Equation 7 as proportional to the measured salinity gradient. Unfortunately, we do not have sufficient velocity data with which to determine du/dz. Therefore, we consider this term to be a constant, and the effects of its variation become a source of unexplained model error. Applying these assumptions, Equation 7 is approximated by

$$Ri = c(\Delta S) \tag{8}$$

where c is a constant of proportionality and ΔS is the salinity difference between the surface and bottom layers. Using this approximation together with Equation 6, the vertical exchange rate can be written as

$$R_v = \frac{k'_v}{(1 + b\Delta S)^{3/2}}(C_u - C) \tag{9}$$

where b is a constant equal to $c \times a$.

Vertical diffusion in an estuary is generally dominated by turbulent processes (Officer, 1976). However, if molecular diffusion is a non-negligible component of net vertical exchange, k'_v may be a function of temperature. For generality, we allow k'_v to vary with temperature according to the Arrhenius formulation,

$$k'_v(T) = k'_{v20}\theta_v^{T-20} \tag{10}$$

where k'_{v20} is the rate constant at 20 °C, and θ_v is the temperature dependency constant (Bowie *et al.*, 1985; Chapra, 1997). Substituting Equations 3 and 9 into Equation 2 yields the full parameterization,

$$\frac{dC}{dt} = -k_d C + \frac{k'_v}{(1 + b\Delta S)^{3/2}}(C_u - C) \tag{11}$$

where k_d and k'_v have temperature dependencies according to Equations 4 and 10.

Equation 11 is a differential equation expressed in terms of t, ‘ time since the last vertical mixing event ’. Unfortunately, measurements do not exist of this critical quantity. However, by relating t to an observed system variable, empirical parameter estimates can still be developed. The continuous time-series of salinity measurements suggests that salinity gradient grows approximately linearly from zero with time after a major vertical mixing event according to,

$$\Delta S = rt \tag{12}$$

where r is the rate of increase (d^{-1}) and ΔS and t are as previously defined. While this rate of increase may vary between stratification events depending on flow and other conditions, an average rate captures aggregate system behaviour. The short duration of the continuous time-series prevents direct estimation of r from the data. However, the value of r can be indirectly estimated by comparing the observed frequency of salinity gradients from the weekly/biweekly data with an estimated frequency of times between vertical mixing events. This frequency-based approach is consistent with the probabilistic model of hypoxia described in the next section.

If extreme wind and flow conditions are assumed to be the mechanisms of vertical mixing, the occurrence of mixing events can be modeled by a Poisson process (Devore, 1991), with the number of mixing events occurring in any time interval assumed to be independent of the number occurring prior to this interval. Under this assumption, the frequency distribution of time between mixing events is represented by an exponential density function,

$$f(t|\lambda) = \lambda e^{-\lambda t} \tag{13}$$

where λ is the rate parameter and $1/\lambda$ is the average time between events. Using the expert elicitation technique described in Morgan and Henrion (1990), a frequency distribution representing the number of days between mixing events was assessed from one of the authors (R. Luettich). His assessments were based on experience with circulation and transport including flow profiles, mid-channel observation, and wind measurements in the Neuse Estuary. The elicitation method we used was based on a series of questions to Luettich aimed at establishing points on the cumulative distribution function (CDF). The fixed value approach (Morgan & Henrion, 1990) was used in a frequency context in order to minimize assessment bias (Anderson, 1998). A typical question was, ‘ If you were to observe 100 vertical mixing events, what is your assessment of the number that would be less than

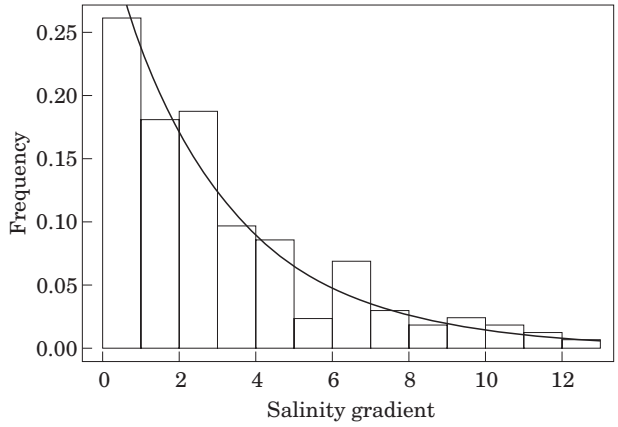

FIGURE 6. Histogram of observed values of salinity gradient at RM9, disregarding the lowest 2/9 of the values. The curve represents an exponential probability density function with rate parameter, λ_s=0·32.

x days apart '. The resulting CDF was best described by an exponential distribution with an average time between mixing events of seven days and a duration of mixing events of two days. Using this estimate, the distribution of time between mixing events becomes,

$$p\ (t=0)=2/9$$
$$f(t|\lambda)=(7/9)\lambda e^{-\lambda t} \quad t>0 \qquad (14)$$

where λ=1/7. Substituting Equation 12 into Equation 14 and normalizing gives,

$$p(\Delta S=0)=2/9$$
$$f(\Delta S|\lambda)=(7/9)\lambda/r\ e^{-\lambda\Delta S/r} \quad S>0 \qquad (15)$$

Thus, after disregarding the lowest 2/9 of the observed values which are assumed to have been collected while a mixing event was occurring, the salinity gradient, ΔS, can be expected to have an exponential distribution with rate parameter λ_s ($=\lambda/r$). At RM9, the lowest 2/9 of the values corresponded to those with $\Delta S \leq 0{\cdot}1$. The remaining values were fit using the distribution fitting capability of Crystal Ball® software (Decisioneering Inc., 1996), resulting in an estimate for the rate parameter, λ_s, of 0·32 (Figure 6). This yielded an estimated average value for r of 0·143/0·32=0·45.

Substituting Equation 12 into Equation 11 gives the dissolved oxygen rate relation in terms of the observed variable, ΔS,

$$\frac{dC}{d\Delta S}=-\frac{k_d}{r}C+\frac{k'_v}{r(1+b\Delta S)^{3/2}}(C_u-C) \qquad (16)$$

To solve Equation 16 we expressed the initial value of the oxygen concentration in the lower water column (at $\Delta S=t=0$) as an unknown percent, $100p$, of C_u, to be estimated from the data. Because the initial condition represents a well-mixed water column, the value of p is expected to be near one. Solving Equation 16 yields,

$$C(\Delta S)=C_u\exp\left(\frac{-k_d\Delta S}{r}+\frac{2k'_v}{br\sqrt{1+b\Delta S}}\right)\times\left[p\times\exp\left(\frac{-2k'_v}{br}\right)+\frac{k'_v}{r}\int_0^{\Delta S}\frac{\exp\left[\frac{k_d x}{r}-\left(\frac{2k'_v}{br\sqrt{1+b\Delta S}}\right)\right]}{(1+bx)^{3/2}}dx\right] \qquad (17)$$

Together with Equations 4 and 10, Equation 17 relates the observed variables, C, C_u, ΔS, and T through the parameters k_{d20}, θ_d, k'_{v20}, θ_v, p, and b, all of which can be estimated from the available data.

Parameter estimation methods

Parameter estimation was performed using the nonlinear least squares routine included in S-Plus® (Chambers & Hastie, 1992). To prevent the routine search method from entering portions of the parameter space in which Equation 17 is undefined, k_{d20} and k'_{v20} were reparameterized as $\exp[k''_{d20}]$ and $\exp[k''_{v20}]$, where k''_{d20} and k''_{v20} equal $\ln(k_{d20})$ and $\ln(k'_{v20})$ respectively. This reparameterization assured that the rate constants as expressed in Equation 16 would maintain positive values. The parameters k''_{d20} and k''_{v20} were assumed to have normal distributions, and the mean, m, and standard error, se, were estimated. This implies that in their original metrics, k_{d20} and k'_{v20} each have lognormal distributions. Because of the skewness of the lognormal distribution, the median was chosen as an indication of the centre of the distribution, and the 95% confidence interval was chosen as an indication of spread. For a lognormally distributed parameter, β, these are calculated as,

$$\mathrm{Med}(\beta)=\exp(m),\ \text{and}$$
$$\mathrm{C.I.}_{95\%}=\exp(\mu\pm 1{\cdot}96\mathrm{SE}) \qquad (18)$$

(Crow & Shimizu, 1988).

For a normally distributed parameter, the median is equal to the mean and the 95% confidence interval is the unexponentiated form of Equation 18.

TABLE 1. Least squares parameter estimates for RM9

Model parameter	Estimated value (median)	95% Confidence interval
k_{d20}	0·113	(0·075, 0·171)
θ_d	1·13	(1·08, 1·18)
k'_{v20}	0·052	(0·010, 0·276)
θ_v	0·986	(0·895, 1·08)
b	−0·012	(−0·124, 0·101)
p	0·933	(0·893, 0·973)

Error sum of squares=493·1; df=219; R^2=0·791.

Model simplification

The empirically parameterized process-based model was found to fit the data at RM9 very well (Table 1). The R^2 value indicates that approximately 79% of the variation in oxygen concentration is described by the model. Furthermore, examination of the empirical parameter estimates suggests that some additional model simplification may be appropriate. The estimated value of θ_v is very close to one, indicating that the temperature dependence of the vertical exchange coefficient is minor. This implies that temperature-insensitive turbulent processes dominate temperature-sensitive molecular processes, as expected in an estuary. The estimation of p is also close to one, implying that the lower water column oxygen concentration upon mixing is close to the oxygen concentration in the surface layer, as expected. In addition, the estimated value of b is very close to zero, indicating that the influence of the salinity gradient on reoxygenation is apparently minor. Examination of Equation 7 reveals a possible explanation. The assumption made in developing Equation 8 was that all terms other than $d\rho/dz$ in Equation 7 could be considered independent of ΔS. In reality, the gradient of horizontal velocity with depth, or shear, is likely to increase as the salinity difference between the layers increases, at least partially offsetting the effects of differences in buoyancy. The result is that although ΔS may vary, Ri may be relatively constant, and the vertical exchange coefficient may be considered to be a constant with respect to ΔS, consistent with an estimated value of b close to zero.

To determine whether simplification of the process-based model is desirable, we used the extra sum of squares F-test. For nested nonlinear models, this test is preferable to a t-test for judging whether restricted models with fixed parameters are preferable to the unrestricted form (Bates & Watts, 1988). The F statistic is calculated as:

TABLE 2. Model F statistics as compared to unrestricted model for RM9

	Model restriction			
	θ_v=1	p=1	b=0	θ_v=1, b=0
Error sum of squares	493·4	517·1	493·3	493·3
df	220	220	220	221
F statistic	0·133	10·6[a]	0·089	0·044

[a]Significant at the 0·01 level.

$$\frac{(ess_r - ess_u)/(df_r - df_u)}{mse_u} \sim F_{df_r - df_u, df_u} \tag{19}$$

where ess_r and ess_u are the restricted and unrestricted error sums of squares, respectively, df_r and df_u are the restricted and unrestricted degrees of freedom, respectively, and mse_u is the mean squared error of the unrestricted model ($mse_u = ess_u/df$). Simplification is appropriate if restricted forms of the model do not result in an error sum of squares that is significantly higher than that of the unrestricted form, as indicated by the F-statistic.

Results of the F-tests (Table 2) indicate that the best-fit model is one in which b is restricted to zero and θ_v is restricted to one, but p is left as a free parameter. The restricted form of Equation 11 then becomes:

$$\frac{dC}{d\Delta S} = -\frac{k_d}{r}C + \frac{k''_v}{r}(C_u - C) \tag{20}$$

where k''_v is neither a function of salinity gradient nor temperature. This rate relation has the computationally simpler analytic solution,

$$C = \frac{C_u\left[p(k''_v + k_d) + k''_v\left\{\exp\left(\frac{(k''_v + k_d)\Delta S}{r}\right) - 1\right\}\right]}{(k''_v + k_d)\exp\left(\frac{(k''_v + k_d)\Delta S}{r}\right)} \tag{21}$$

Model results and discussion

Process rates estimated for the best-fit model (Table 3) are generally consistent with values reported previously for the Neuse and other partially mixed estuaries. For eight mid-estuarine locations in the Neuse, measurements of benthic oxygen demand made in a laboratory chamber at 20 °C and an oxygen concentration of 6·0 mg l^{-1} were reported to have a mean of 0·70 g m^{-2} d^{-1} and a standard deviation of 0·16 g m^{-2} d^{-1} (Alperin *et al.*, 1998). *In situ* sediment measurements taken at six locations with varying

TABLE 3. Least squares parameter estimates for best-fit model at RM9

Model parameter	Estimated value (median)	95% Confidence interval
k_{d20}	0·114	(0·086, 0·151)
θ_d	1·13	(1·11, 1·16)
k''_v	0·058	(0·029, 0·114)
p	0·932	(0·893, 0·971)

Residual standard error = 1·49; R^2 = 0·791.

temperature and oxygen concentration were reported to be $0{\cdot}90 \pm 0{\cdot}38\ g\ m^{-2}\ d^{-1}$ (Sauber, 1998). To date, measurements of net diurnal lower water column oxygen demand in the Neuse have not been made. By using monitoring data to empirically estimate net consumption rates, our model captures the sum of benthic and pelagic processes. Additionally, use of field data in estimating oxygen budgets may better represent long-term field conditions by inherently integrating over time and space (Kemp & Boynton, 1980; Swaney *et al.*, 1999). Assuming a lower water column thickness of 1·5 m (Alperin *et al.*, 1998) our empirically estimated oxygen consumption rate constant, k_{d20}, corresponds to a combined benthic and integrated lower water column oxygen demand of $1{\cdot}02\ g\ m^{-2}\ d^{-1}$ at an oxygen concentration of $6{\cdot}0\ mg\ l^{-1}$. When compared to the laboratory and field measurements of sediment oxygen demand, this result suggests that benthic processes compose the bulk of the oxygen depletion rate, and net water column demand is relatively minor. This may be a general result for shallow, stratified systems (Kemp *et al.*, 1992). While temperature effects on respiration have not been previously explored for the Neuse, values for θ reported in the literature range from 1·02 to 1·13 (Bowie *et al.*, 1985). The model-derived value falls at the high end of this range.

The estimated vertical exchange coefficient, k''_{v20}, corresponds to a reoxygenation rate of $0{\cdot}69\ g\ m^{-2}\ d^{-1}$ when the oxygen gradient is $6{\cdot}0\ mg\ l^{-1}$. Although measurements of this quantity have not been made for the Neuse, our value is in agreement with values estimated for other systems under stratified conditions (Kemp & Boynton, 1980; Bulleid, 1983; Kemp *et al.*, 1992).

Overall system behaviour can be best depicted by a surface representing predictions of dissolved oxygen concentration as a function of time since the last mixing event and water temperature. Because oxygen concentration in the upper water column is generally at saturation, C_u can be related to water temperature according to the empirical formula (Hyer *et al.*, 1971),

$$C_u = 13{\cdot}686 - 0{\cdot}34663T + 0{\cdot}00450T^2 \qquad (22)$$

assuming an average salinity of 10. This relationship allows bottom water oxygen to be expressed as a function of time and water temperature alone. Salinity effects were not explicitly included in Equation 22, because they are relatively minor compared to the effects of temperature, and, unlike water temperature, salinity is not predictable. Therefore, any effects of salinity changes become part of the variance not explained by the model.

The shape of the prediction surface (Figure 7) shows that dissolved oxygen decreases exponentially with time after a mixing event and that the rate of this decrease increases at higher temperature. As Equation 20 indicates, the rate of change of oxygen concentration is determined by the relative magnitudes of oxygen demand and reoxygenation. At low temperature, the oxygen demand coefficient is low and the vertical exchange coefficient is relatively high, such that the two processes are nearly in balance and dissolved oxygen remains at high levels, even under extended periods of stratification. At higher temperature, the initial oxygen concentration is lower due to changes in the saturation value. Additionally, the oxygen demand increases and dominates reoxygenation, such that dissolved oxygen in the lower layer decreases rapidly. However, as the vertical oxygen gradient grows, reoxygenation increases and the rates of the two processes eventually reach equilibrium. The result is that an oxygen concentration less than $4\ mg\ l^{-1}$ is only expected under extended periods without mixing at a temperature exceeding 15 °C, while a concentration less than $2\ mg\ l^{-1}$ is only expected when temperature exceeds 20 °C.

Comparison of process rates across locations

To test the generality of our results, we applied the process-based model in Equation 22 to the data collected at RM15. We assumed that the mixing rate would be the same at the two stations due to their proximity and the similar orientation of the channel at these two locations. However, because the salinity gradient values at RM15 were best fit by an exponential distribution with rate parameter equal to 0·22 (not shown), the value of r was modified to be 0·64. This higher value implies that stratification sets up more quickly after a wind mixing event at RM15 than at RM9, perhaps due to its proximity to the source of freshwater flow. To accommodate differences caused

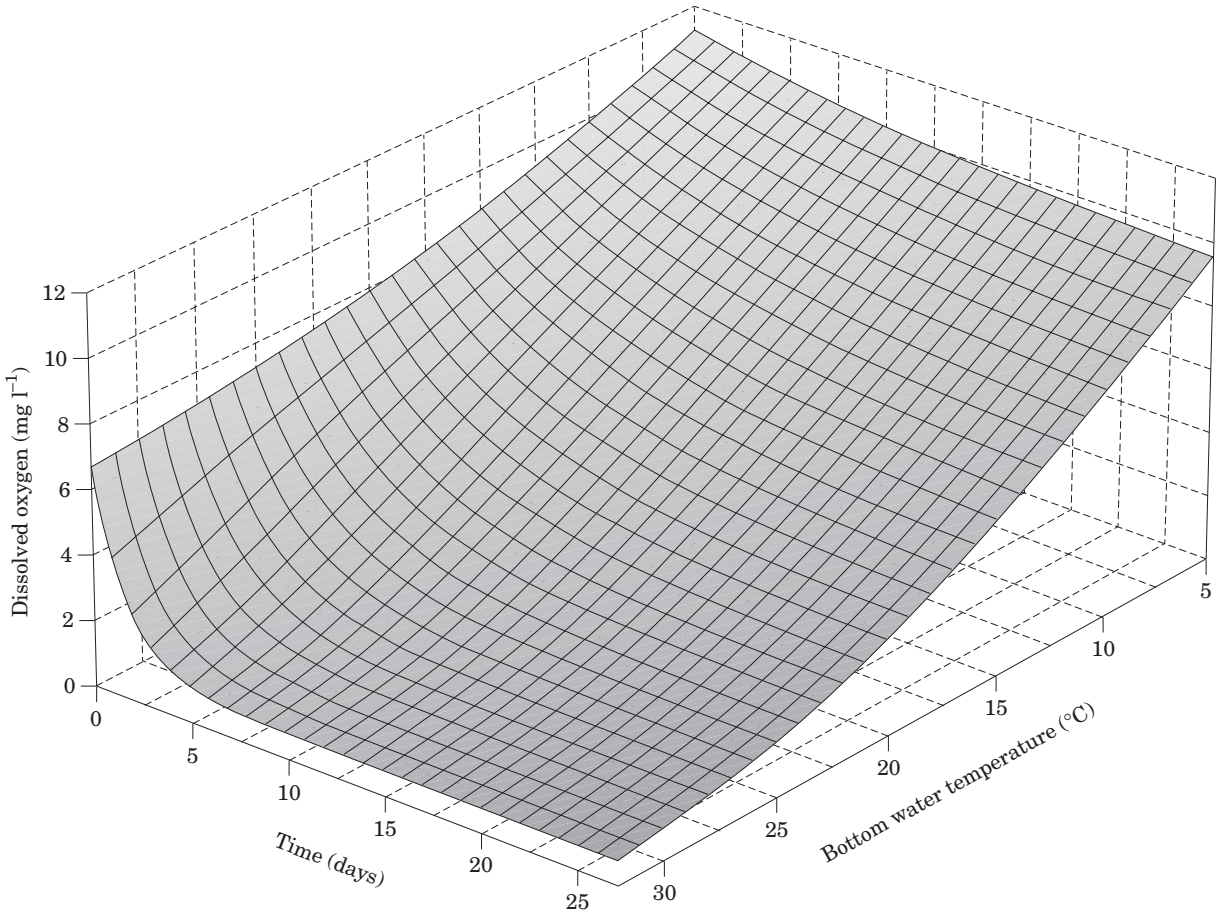

FIGURE 7. Surface representing predicted dissolved oxygen values at RM9 over the range of observed bottom water temperatures and salinity gradients.

by flow and bathymetry, the remaining parameters were allowed to differ by location.

Estimated parameter values for RM15 (Table 4) are similar to those estimated for RM9. After accounting for the reduced depth at this location (bottom layer thickness assumed to be 1 m) estimates of oxygen demand and vertical exchange rate are nearly identical. This is consistent with the findings of Alperin *et al.* (1998) which note minor variation in oxygen demand among mid-estuary locations. Model fit is also similar, as indicated by the high R^2 value, indicating that the model is robust with respect to location.

TABLE 4. Least squares parameter estimates for RM15

Model parameter	Estimated value (median)	95% Confidence interval
k_{d20}	0·186	(0·140, 0·247)
θ_d	1·12	(1·09, 1·14)
k''_{v20}	0·072	(0·036, 0·142)
p	0·959	(0·901, 1·01)

Residual standard error = 1·54; R^2 = 0·778.

Short term oxygen dynamics and model verification

Our model was fit to weekly/biweekly data because they were collected at regular intervals over a number of years. However, these data do not lend insight into the ability of the model to reproduce short-term oxygen dynamics. To address this issue, we applied the model to a set of daily data collected intermittently since 1989 by the U.S. Geological Survey. This data set consists of 1101 daily observations of salinity, temperature, and oxygen concentration in the surface and bottom layers at RM9. Of these 1101 observations, 784 were collected in different years from the weekly/biweekly data, while most of the remainder were necessarily collected on different days because of the difference in sampling frequency. Therefore, this data set provides an opportunity for model verification.

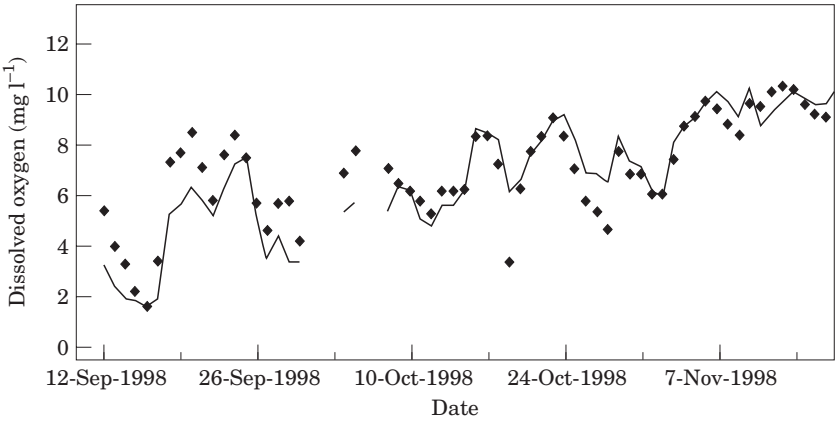

FIGURE 8. A representative two-month period of verification data comparing predicted (line) and observed (points) bottom water oxygen concentrations.

The model parameters estimated from the weekly/biweekly data for RM9 (Table 3) were used in Equation 21 to predict bottom water oxygen concentration for the days corresponding to the daily USGS data. The overall model fit can be measured by the R^2 value of 0·704 and the residual standard error of 1·67 mg l^{-1}. Considering that model parameters were not optimized to this verification data set, these reasonable results increase our confidence in applying the model to new time periods.

A representative two-month time period comparing predicted and observed oxygen concentrations (Figure 8) reveals the ability of the model to represent the short-term dynamics of oxygen depletion. The time-series shows periods of declining bottom water oxygen concentration periodically interrupted by mixing events which bring the concentration back near saturation. As the water cools throughout this autumn period, the rate of depletion can be seen to decrease, while the saturation value increases. There is clearly some scatter in the data around the model predictions, however the model appears to reasonably represent both short-term changes and longer-term seasonal behaviour.

Probabilistic prediction

Monte Carlo methodology

Given our inability to anticipate precisely when mixing events will occur or exactly what the water temperature will be, even with a well parameterized model we cannot expect to be able to make predictions of the bottom water oxygen concentration for any given day. This is a problem encountered whenever a deterministic model is employed. If it is assumeed, however, that the mechanisms that drive vertical mixing and temperature variation will remain the same into the future, values for these predictors can be described by a probability distribution for a time period of interest. The uncertainty in estimated parameter values, as well as overall model uncertainty, can also be described by probability distributions. For a relatively simple model, such as the one described here, Monte Carlo simulation can then be used to generate probabilistic predictions for quantities of interest such as the number of days of hypoxia expected in a given season (Reckhow & Chapra, 1999).

Monte Carlo simulation was performed on the oxygen depletion model using Crystal Ball® (Decisioneering Inc., 1996), a commercially available add-in for Microsoft Excel®. In specifying the distributions for the Monte Carlo simulation, the results for RM9 were used. Therefore, model predictions relate to oxygen concentration at the location in the estuary near RM9. Recent studies of aquatic habitat in the Neuse have noted natural breakpoints in habitat availability at 2 and 4 mg l^{-1} (Eby *et al.*, 1999). Therefore, we have assessed model predictions with these values as criteria. Because hypoxia is most frequent in the summer, assessments focused on the summer season.

Model parameters were assigned the appropriate normal or lognormal distributions with means, standard errors, and correlations determined from the least squares estimation procedure (Tables 3 and 5). Water temperature was assigned a mixture distribution composed of three data-based month-specific normal distributions for July, August and September (Table 6). Based on the distribution of weekly/biweekly surface measurements (not shown), oxygen concentration in the upper layer is described as a normally distributed percent saturation with a mean equal to 100% and a standard deviation equal to 14%

TABLE 5. Parameter correlations for RM9

	$\ln(k_{d20})$	θ_d	$\ln(k''_{v20})$
θ_d	−0·347		
$\ln(k''_{v20})$	0·884	−0·386	
p	0·509	−0·299	0·351

TABLE 6. Monthly bottom water temperature distributions at RM9

	Mean	SD
July	27·88	0·91
August	27·51	1·46
September	24·69	1·89

and was calculated from water temperature according to Equation 23. Time since the last vertical mixing event was assigned the modified exponential distribution given in Equation 14. In addition to parameter and input uncertainties, an additive error term was included to account for the variability in oxygen concentration not explained by the model. This error term captures the effect of simplifications made in model formulation and has a normal distribution with mean equal to zero and standard deviation equal to the residual standard error estimated for the model (Table 3). A histogram of the model residuals (not shown) supported the normality assumption.

Probabilistic predictions for the summer season were generated by using the Monte Carlo method to draw 10 000 sets of predictor variables, parameter values, and error terms, each of which was used to calculate a predicted oxygen concentration according to the model. The distribution of these oxygen values corresponds to the model-predicted oxygen concentration for any given summer day, including the uncertainty associated with parameter error, model error, and natural variability in the predictor variables. From this set of values, 10 000 sample sets of size 90 were drawn with replacement. Called ' bootstrapping ' (Efron & Tibshirani, 1993), this procedure was used to simulate the interannual variability in observed daily oxygen concentration. For each set of 90 days, the number of days with predicted oxygen concentration less than 2 mg l^{-1} and less than 4 mg l^{-1} were recorded.

Monte Carlo results

The Monte Carlo simulation indicates that the number of days in a given summer at RM9 with oxygen concentration less than 2 mg l^{-1} is predicted to have an average of 23·8 (or 26%). Because of both model uncertainty and interannual variability, this value varies with a standard deviation of 4·2 days [Figure 9(a)]. The average of the predicted number of days with concentration less than 4 mg l^{-1} is 46·8 (52%) with a standard deviation of 4·7 [Figure 9(b)]. For reference, 21 out of the 66 weekly/biweekly DO observations taken during the summer at RM9 had values less than 2 mg l^{-1} (31%) and 27 had values less than 4 mg l^{-1} (41%). Accounting for the size of the observed sample, the proportions predicted by the model and those calculated from the data are not significantly different at the 0·05 level (Devore, 1991). Model predictions also compare favourably with a spatially-distributed sampling scheme conducting during the summers of 1997 and 1998 (Eby *et al.*, 1999) which found an average of 25% of the middle portion of the estuary to have an oxygen concentration below 2 mg l^{-1} and 50% to be below 4 mg l^{-1}.

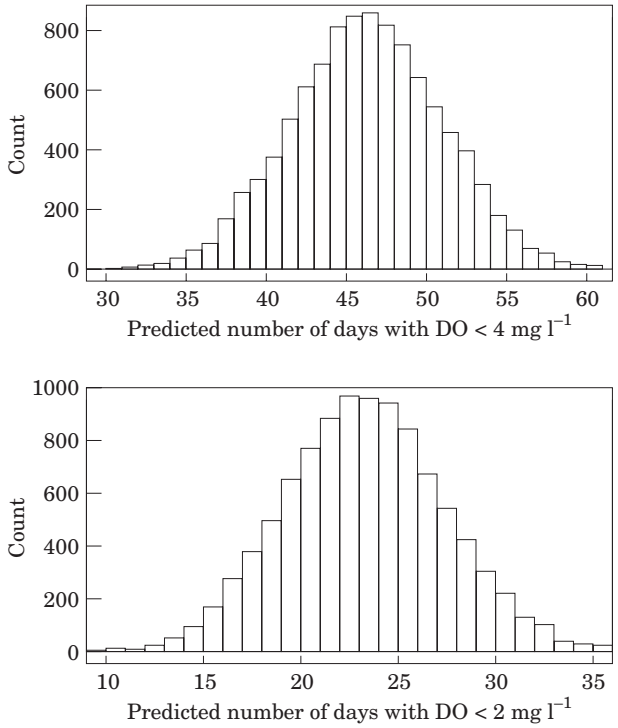

FIGURE 9. Histogram of the predicted number of days during the summer season with dissolved oxygen concentration (a) ≤2 mg l^{-1} and (b) ≤4 mg l^{-1}. One thousand seasons of 90 days each were simulated.

Discussion

The empirically parameterized oxygen model is appealing in its ability to describe a large fraction of

the observed variability in oxygen concentration. Additionally, the derived process rates represent aggregate system behaviour in a way that is not captured by laboratory and field measurements. Simplifying assumptions were made in model specification to maintain a consistency between model detail and the availability of data. However, when predictions are expressed probabilistically, the effects of any processes not currently considered in the model are not ignored but become part of the prediction uncertainty. Perhaps, if sufficient future observations can be made to add additional detail to the model, a portion of the remaining 21% variability in oxygen concentration can be described. Candidates for predictor variables include a time-lagged algal productivity value, local flow measurements, and wind speed and direction.

A distinguishing feature of our oxygen model is its explicit use of expert judgment in relating salinity gradient to time. While this assessment technique may appear to be a subjective process, it must be kept in mind that all modelling implicitly involves personal judgment, whether in model formulation, parameter selection, or the interpretation of results. In general, we minimize subjectivity by estimating parameter values directly from observational data. However, when sufficient data do not exist for empirical parameter estimation, as is the case for the parameter r, we formalize the assessment process by using established techniques of eliciting the value of an uncertain quantity and describing the associated uncertainty with a probability distribution. In this case, the assessed distribution of time between mixing events was of a form consistent with probability theory, thus supporting the applicability of the method. Because the parameter r is only used in relating salinity gradient to time, errors in its assessment would affect our interpretation of the rate constants in Equation 20, but would not impact model fit nor predictive ability.

The model developed in this study relates benthic and lower water column oxygen demand to the frequency of bottom water hypoxia. To predict the effects of nutrient management actions on estuarine conditions, the oxygen demand rate currently used in the model can be replaced with a value estimated to result from a long-term reduction in nutrient loading and phytoplankton growth. If such an assessment is also performed in a probabilistic manner, integrated predictions of oxygen conditions can be made that account for scientific uncertainty and natural variability. Such probabilistic predictions provide more realistic assessments than single-values and allow for the value of additional research and monitoring to be made based on the degree to which such work can reduce predictive uncertainty. The authors are currently pursuing modelling work along these lines.

Acknowledgements

We are grateful to Robert Christian and Donald Stanley at East Carolina University for making their data available for this analysis. We also thank Gabriel Katul and David Higdon for assistance with mathematical and statistical methods and Kenneth Reckhow, Robert Christian, and Christopher Buzzelli for critical reviews of the manuscript. This work was supported by a grant from the Water Resources Research Institute of the University of North Carolina.

References

Alperin, M. J., Clesceri, E. J., Wells, J. T., Albert, D. B., McNinch, J. E. & Martens, C. S. 1998 Neuse River Estuary modeling and monitoring project final report: Monitoring phase, Ch. 5: Sedimentary processes and benthic-pelagic coupling. *Prepared for the Water Resources Research Institute of the University of North Carolina*, pp. 63–105.

Anderson, J. L. 1998 Embracing uncertainty: The interface of Bayesian statistics and cognitive psychology. *Conservation Ecology* (on line) **2,** 2.

Bates, D. M. & Watts, D. G. 1988 *Nonlinear regression analysis and its applications*. Wiley and Sons, New York, NY. 365 pp.

Bowie, G. L., Mills, W. B., Porcella, D. B., Campbell, C. L., Pagenkopf, J. R., Rupp, G. L., Johnson, K. M., Chan, P. W. H., Gherini, S. A. & Chamberlin, C. E. 1985 Rates, constants, and kinetic formulations in surface water quality modeling (Second Edition). U.S. Environmental Protection Agency, ORD, Athens, GA, ERL, *EPA/600/3-85/040*. 455 pp.

Boyer, J. N., Stanley, D. W. & Christian, R. R. 1994 Dynamics of NH_4^+ and NO_3^- uptake in the water column of the Neuse River Estuary, North Carolina. *Estuaries* **17,** 361–371.

Bulleid, N. C. 1983 The nutrient cycle of an intermittently stratified estuary. In *Synthesis and Modelling of Intermittent Estuaries* (Cuff, W. R. & Tomczak, M. Jr., eds). Springer, New York, NY. pp. 55–75.

Chambers, J. M. & Hastie, T. J. 1992 *Statistical models in S*. Wadsworth and Brooks/Cole, Pacific Grove, CA. 608 pp.

Chapra, S. C. 1997 *Surface water-quality modeling*. WCB/McGraw-Hill, Boston, MA. 844 pp.

Christian, R. R., Bryant, W. L. & Stanley, D. W. 1986 The relationship between river flow and Microcystis aerunginosa blooms in the Neuse River, North Carolina. Water Resources Research Institute of the University of North Carolina, Raleigh, NC. *Report No. 223*.

Crow, E. L. & Shimizu, K. 1988 *Lognormal distributions: theory and applications*. Marcel Dekker, New York, NY. 387 pp.

Dauer, D. M., Rodi, A. J. & Ranasinghe, J. A. 1992 Effects of low dissolved-oxygen events on the macrobenthos of the lower Chesapeake Bay. *Estuaries* **15,** 384–391.

Decisioneering Inc. 1996 *Crystal Ball*. Version 4.0 Computer program manual. 286 pp.

Devore, J. L. 1991 *Probability and statistics for engineering and the sciences*. Brooks/Cole, Pacific Grove, CA. 716 pp.

Diaz, R. J. & Rosenberg, R. 1995 Marine benthic hypoxia: a review of its ecological effects and the behavioural responses of benthic macrofauna. *Oceanography and Marine Biology* **33,** 245–303.

Eby, L., Crowder, L. & McClellan, C. 1999 Neuse River Estuary modeling and monitoring project final report: Fish distribution and habitat. *Prepared for the Water Resources Research Institute of the University of North Carolina*.

Efron, B. & Tibshirani, R. 1993 *An Introduction to the Bootstrap*. Chapman and Hall, New York, NY. 436 pp.

Geyer, W. R. 1993 The importance of suppression of turbulence by stratification on the estuarine turbidity maximum. *Estuaries* **16,** 113–125.

Godfrey, J. S. 1983 Tidal flushing and vertical diffusion in South West Arm, Port Hacking. In *Synthesis and modelling of intermittent estuaries* (Cuff, W. R. & Tomczak, M. Jr., eds). Springer, New York, NY, pp. 27–54.

Hastie, T. J. & Tibshirani, R. J. 1990 *Generalized additive models*. Routledge, Chapman and Hall, New York, NY. 335 pp.

Hyer, P. V., Fang, C. S., Ruzecki, E. P. & Hargis, W. J. 1971 *Hydrography and hydrodynamics of Virginia esuaries, studies of the distribution of salinity and dissolved oxygen in the Upper York System*. Virginia Institute of Marine Science.

Kemp, W. M. & Boynton, W. R. 1980 Influence of biological and physical processes on dissolved oxygen dynamics in an estuarine system: Implications for measurement of community metabolism. *Estuarine Coastal and Marine Science* **11,** 407–431.

Kemp, W. M., Sampou, P. A., Garber, J., Tuttle, J. & Boynton, W. R. 1992 Seasonal depletion of oxygen from bottom waters of Chesapeake Bay—roles of benthic and planktonic respiration and physical exchange processes. *Marine Ecology Progress Series* **85,** 137–152.

Kuo, A. Y., Park, K. & Moustafa, M. Z. 1991 Spatial and temporal variabilities of hypoxia in the Rappahannock River, Virginia. *Estuaries* **14,** 113–121.

Lohrenz, S. E., Fahnenstiel, G. L., Redalje, D. G., Lang, G. A., Chen, X. G. & Dagg, M. J. 1997 Variations in primary production of northern Gulf of Mexico continental shelf waters linked to nutrient inputs from the Mississippi River. *Marine Ecology Progress Series* **155,** 45–54.

Luettich, R. A., McNinch, J. E., Pinckney, J. L., Alperin, M., Martens, C. S., Paerl, H. W., Peterson, C. H. & Wells, J. T. 1998 Neuse River Estuary modeling and monitoring project final report: Monitoring phase, Ch. 2: Field setting. *Prepared for the Water Resources Research Institute of the University of North Carolina*. pp. 4–5.

McMahon, G. & Woodside, M. D. 1997 Nutrient mass balance for the Albemarle-Pamlico drainage basin, North Carolina and Virginia, 1990. *Journal of the American Water Resources Association* **33,** 573–589.

McNinch, J. E. & Luettich, R. A. Jr. 1998 Neuse River Estuary modeling and monitoring project final report: Monitoring phase, Ch. 3: Hydrography and circulation. *Prepared for the Water Resources Research Institute of the University of North Carolina*, pp. 5–43.

Moore, B. C., Chen, P.-H., Funk, W. H. & Yonge, D. 1996 A model for predicting lake sediment oxygen demand following hypolimnetic aeration. *Water Resources Bulletin* **32,** 723–731.

Morgan, M. G. & Henrion, M. 1990 *Uncertainty: A guide to dealing with uncertainty in quantitative risk and policy analysis*. Cambridge University Press, Cambridge, UK. 332 pp.

Munk, W. H. & Anderson, E. R. 1948 Notes on a theory of the thermocline. *Journal of Marine Research* **7,** 276–295.

Nixon, S. W. 1981 Remineralization and Nutrient Cycling in Coastal Marine Ecosystems. In *Estuaries and Nutrients* (Neilson, B. J. & Cronin, L. E., eds). Humana, pp. 111–138.

North Carolina Department of Environment, Health and Natural Resources 1993 *Neuse River Basinwide Water Quality Management Plan*. Raleigh, NC. 214 pp.

Officer, C. B. 1976 *Physical Oceanography of Estuaries*. John Wiley and Sons, New York, NY. 465 pp.

Officer, C. B., Biggs, R. B., Taft, J. L., Cronin, L. E., Tyler, M. A. & Boynton, W. R. 1984 Chesapeake Bay anoxia: Origin, development and significance. *Science* **223,** 22–27.

Paerl, H. W., Mallin, M. A., Donahue, C. A., Go, M. & Peierls, B. L. 1995 Nitrogen loading sources and eutrophication of the Neuse River estuary, North Carolina: direct and indirect roles of atmospheric deposition. Water Resources Research Institute of the University of North Carolina. *Report No. 291*. Raleigh, NC.

Paerl, H. W., Pinckney, J. L., Fear, J. M. & Peierls, B. L. 1998 Ecosystem responses to internal and watershed organic matter loading: consequences for hypoxia in the eutrophying Neuse River Estuary, North Carolina, USA. *Marine Ecology Progress Series* **166,** 17–25.

Park, S. S. & Jaffe, P. R. 1999 A numerical model to estimate sediment oxygen levels and demand. *Journal of Environmental Quality* **28,** 1219–1226.

Phoel, W. C., Webb, K. L. & D'Elia, C. F. 1981 Inorganic nitrogen regeneration and total oxygen consumption by the sediments at the mouth of the York River, Virginia. In *Estuaries and Nutrients* (Neilson, B. J. & Cronin, L. E., eds). Humana, pp. 607–618.

Pihl, L., Baden, S. P., Diaz, R. J. & Schaffner, L. C. 1992 Hypoxia-induced structural changes in the diet of bottom-feeding fish and crustacea. *Marine Biology* **112,** 349–361.

Reckhow, K. H. 1994*a* Water quality simulation modeling and uncertainty analysis for risk assessment and decision making. *Ecological Modelling* **72,** 1–20.

Reckhow, K. H. 1994*b* Importance of scientific uncertainty in decision making. *Environmental Management* **18,** 161–166.

Reckhow, K. H. & Qian, S. S. 1994 Modeling phosphorus trapping in wetlands using generalized additive models. *Water Resources Research* **30,** 3105–3114.

Reckhow, K. H. 1999 Water quality prediction and probability network models. *Canadian Journal of Fisheries and Aquatic Sciences* **56,** 1150–1158.

Reckhow K. H. & Chapra, S. C. 1999 Modeling excessive nutrient loading in the environment. *Environmental Pollution* **100,** 197–207.

Rizzo, W. M. & Christian, R. R. 1996 Significance of subtidal sediments to heterotrophically-mediated oxygen and nutrient dynamics in a temperate estuary. *Estuaries* **19,** 475–487.

Sauber, J. 1998 Neuse River internal nutrient loading studies: 1996–1997. *North Carolina Division of Water Quality Initial Report*.

Stanley, D. W. & Nixon, S. W. 1992 Stratification and bottom-water hypoxia in the Pamlico River estuary. *Estuaries* **15,** 270–281.

Swaney, D. P., Howarth, R. W. & Butler, T. J. 1999 A novel approach for estimating ecosystem production and respiration in estuaries: Application to the oligohaline and mesohaline Hudson River. *Limnology and Oceanography* **44,** 1509–1521.

Thomson, E. E. 1998 *Impacts of summer hypoxia on benthic fauna and implications for fisheries productivity in the Neuse River estuary, North Carolina*. M.S. Thesis. University of North Carolina at Chapel Hill.

Turner, R. E., Schroeder, W. W. & Wiseman, W. J. Jr. 1987 The role of stratification in the deoxygenation of Mobile Bay and adjacent shelf bottom waters. *Estuaries* **10,** 13–19.

Walters, C. J. & Holling, C. S. 1990 Large-scale management experiments and learning by doing. *Ecology* **71,** 2060–2068.

Winn, R. N. & Knott, D. M. 1992 An evaluation of the survival of experimental populations exposed to hypoxia in the Savanna River estuary 1992. *Marine Ecology Progress Series* **88,** 161–179.